ACS APPLIED MATERIALS & INTERFACES

Research Article

www.acsami.org

Robust and Biodegradable Elastomers Based on Corn Starch and Polydimethylsiloxane (PDMS)

Luca Ceseracciu,[†] José Alejandro Heredia-Guerrero,[†] Silvia Dante,[‡] Athanassia Athanassiou,[†] and Ilker S. Bayer*[,†]

[†]Smart Materials and [‡]Nanophysics, Istituto Italiano di Tecnologia, Via Morego 30, 16163 Genova, Italy

ABSTRACT: Designing starch-based biopolymers and biodegradable composites with durable mechanical properties and good resistance to water is still a challenging task. Although thermoplastic (destructured) starch has emerged as an alternative to petroleum-based polymers, its poor dimensional stability under humid and dry conditions extensively hinders its use as the biopolymer of choice in many applications. Unmodified starch granules, on the other hand, suffer from incompatibility, poor dispersion, and phase separation issues when compounded into other thermoplastics above a concentration level of 5%. Herein, we present a facile biodegradable elastomer preparation method by incorporating large amounts of unmodified corn starch, exceeding 80% by volume, in acetoxy-polyorganosiloxane thermosets to produce mechanically robust, hydrophobic bioelastomers. The naturally adsorbed moisture on the surface of starch enables autocatalytic rapid hydrolysis of polyorganosiloxane to form Si−O−Si networks. Depending on the amount of starch granules, the mechanical properties of the bioelastomers can be easily tuned with high elastic recovery rates. Moreover, starch granules considerably lowered the surface friction coefficient of the polyorganosiloxane network. Stress relaxation measurements indicated that the bioelastomers have strain energy dissipation factors that are lower than those of conventional rubbers, rendering them as promising green substitutes for plastic mechanical energy dampeners. Corn starch granules also have excellent compatibility with addition-cured polysiloxane chemistry that is used extensively in microfabrication. Regardless of the starch concentration, all of the developed bioelastomers have hydrophobic surfaces with lower friction coefficients and much less water uptake capacity than those of thermoplastic starch. The bioelastomers are biocompatible and are estimated to biodegrade in Mediterranean seawater within three to six years.

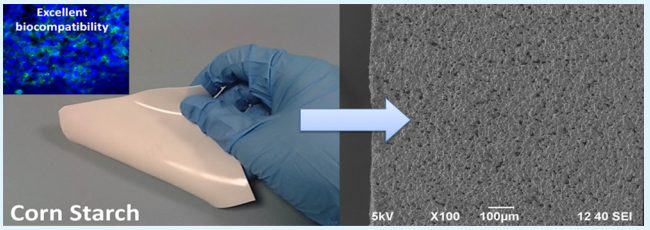

KEYWORDS: *starch, polydimethylsiloxane, biodegradable elastomer, biopolymer*

INTRODUCTION

Starch is a highly abundant and renewable agricultural resource whose industrial production exceeds 7 million tons/year in Europe alone.[1] Half of this production is used for nonfood applications, such as paper sizing, adhesives, biofuels, and bioplastics.[2] The molecular structure of starch consists of a combination of linear macromolecules known as amylose and branched macromolecular chains known as amylopectin. A starch granule is a continuous structure that is made up of regions of amorphous and highly and moderately crystalline zones. The crystalline region is formed by linear fractions of amylopectin, whereas branch points and amylose are the main components of the amorphous zones.[3,4] Starch-based biopolymers are among the most widely studied biomaterials.[5] The most common form of starch in biopolymer technology is known as thermoplastic starch (TPS) or destructured starch.[6] To obtain TPS, starch can be destructured by gelatinization in hot water and then cast into films upon drying. Alternatively, its original structure can be disrupted by simultaneous heating and shearing, resulting in a thermoplastic melt, which can be accomplished with conventional extruders (or similar equipment) used for processing thermoplastics.[7] Unfortunately, TPS is highly susceptible to dimensional instability under both low and high humidity environments. Plasticization with various additives such as glycerol is very common, but plasticized TPS still has very low resistance to water. In a typical plasticized TPS model system, the diffusion of plasticizer out of TPS when exposed to low humidity conditions, and diffusion of water into the product under high humidity conditions, is inevitable and results in poor stability. This causes brittleness due to the loss of plasticizer in a low humidity environment and shape and texture retention issues due to excess absorbed water in a high humidity environment.[8] To circumvent these problems, starch is generally destructured in the presence of other biodegradable polymers, such as vinyl alcohol copolymers, poly(lactic acid)s, aliphatic polyesters, and cellulose derivatives, to name just a few.[9−11] Particularly, thermoformed blends of TPS with biodegradable polyesters like polycaprolactone and poly(lactic acid) are highly popular, and some of these blends have already been commercialized.[12] The use of compatibilizers, however, is still needed to enhance TPS dispersion and minimize interfacial failure.[13]

Received: December 3, 2014
Accepted: January 26, 2015
Published: January 26, 2015

DOI: 10.1021/am508515z
ACS Appl. Mater. Interfaces 2015, 7, 3742−3753

Scheme 1

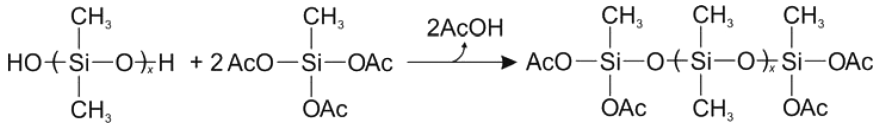

Scheme 2

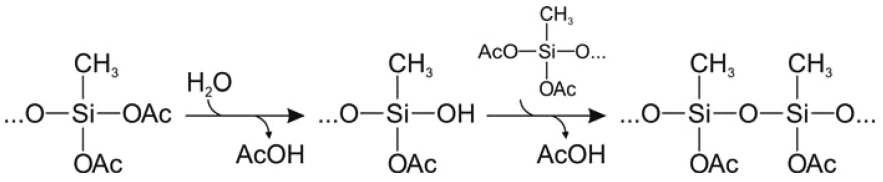

Scheme 3

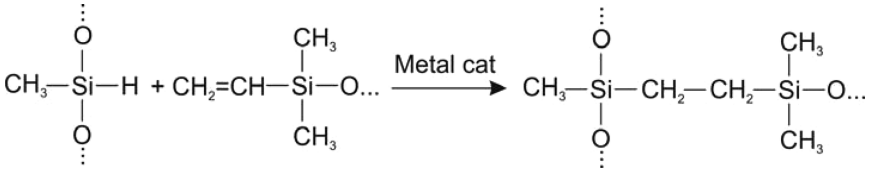

Unmodified (granular) starch, on the other hand, has been proposed to be a sustainable filler material for petroleum-based polymers.[14] However, the use of unmodified starch as a component for polymer compounding is quite challenging due to its large particle size (~20 μm), inherent hydrophilicity, and uptake of moisture. Griffin[15] was the first to introduce biodegradability to synthetic commodity polymers like polyethylene by adding 7−20% granular corn starch modified not through destructuring but by altering the starch surface with a silane coupling agent. The main problem associated with introducing unmodified starch into hydrophobic nondegrading polymers, such as low density polyethylene, is the formation of water bubbles within the polymer matrix, which then degrade the composite mechanical properties of the polymers considerably once the starch concentration level exceeds 15%.[16] These bubbles originate from naturally adsorbed moisture in the unmodified starch. Bubbles can form during extrusion while melting the polymer matrix or after the formation of the composite during storage or use. Therefore, blending starch granules with hydrophobic petroleum thermoplastics generally requires complete particle drying and surface functionalization or modification in the form of grafting or coupling agents.[15,16] A very recent study by Kim and Peterson[17] compounded an ethyl cyanoacrylate (ECA) monomer with unmodified starch granules by up to 60% and molded them into various highly rigid shapes. The natural moisture on the surface of starch initiated polymerization of ECA monomers into poly(ethyl cyanoacrylate). The mechanical strength of the biodegradable composite was comparable to nondegrading petroleum-based polymers, such as polypropylene, polyethylene, and polystyrene.[17]

In this study, we report the fabrication and characterization of biodegradable elastomers (bioelastomers) by incorporating large amounts of unmodified corn starch granules into polyorganosiloxane matrices cross-linked by either condensation (acetoxy-cured) or addition (platinum-cured) in the presence of starch. Cross-linked polyorganosiloxane networks are known to biodegrade in soil through abiotic hydrolysis to monomeric dimethylsilanediols[18−20] and through other mechanisms such as microbiotic degradation and volatilization[21,22] into CO_2 and silica. Acetoxy-polydimethylsiloxane (acetoxy-PDMS) networks formed in this way are known as room temperature vulcanizing silicone elastomers, and they are used in a wide range of applications from electrical insulation to medical prosthetics and plastic surgery.[23] Fabrication requires no complicated equipment or tools and takes place under ambient conditions. The bioelastomers demonstrate hydrophobicity that is high and friction coefficients that are low compared to those of standard silicone rubbers, as well as excellent cell biocompatibility and mechanical energy damping properties. Bioelastomers are also shown to start the biodegradation process in Mediterranean seawater, which was chosen as a model environment.

MATERIALS AND METHODS

Unmodified regular corn starch containing approximately 73% amylopectin and 27% amylose and reagent grade heptane were purchased from Sigma-Aldrich and used as received. Acetoxy-polysiloxane (acetoxy-PDMS, Elastosil E43) was purchased from Wacker Chemie AG and used as received. It is a proprietary mixture of hydroxyl end-blocked polydimethylsiloxane, also known as hydroxyl-terminated polydimethylsiloxane (PDMS), and triacetoxy(methyl)-silane (<10%) using dibutyltin diacetate (<0.1%) as a catalyst. Two-part PDMS Sylgard 184 (platinum-cured) was purchased from Dow Corning and is made up of dimethylvinyl-terminated dimethylsiloxane (~50%), dimethylvinylated and trimethylated silica (~45%), and tetra(trimethylsiloxy)silane (5%). Acetoxy-polyorganosiloxanes are reactive oligomers prepared from hydroxyl end-blocked polyalkyl siloxanes and excess acetoxysilanes such as methyltriacetosilanes. They can be cross-linked by condensation polymerization initiated by contact with moisture[24] as shown in Scheme 1, where Ac denotes -$OCCH_3$ groups.

Once the acetoxy groups are hydrolyzed by ambient moisture to produce silanols, further condensation takes place as shown in Scheme 2.

In Scheme 2, AcOH stands for acetic acid that is released as a byproduct of the reaction during cross-linking.[25] Similarly, addition cross-linking occurs by reacting vinyl-terminated siloxanes with Si−H groups (Scheme 3).

The addition is mainly catalyzed by platinum or ruthenium metal complexes.[24,25] The preferred cure system may vary by application.

DOI: 10.1021/am508515z
ACS Appl. Mater. Interfaces 2015, 7, 3742−3753

For instance, silicone-to-silicone medical adhesives use an acetoxy cure, whereas a Pt cure (siloxy) is used for precise silicone parts.

The fabrication procedure of the bioelastomers was as follows. Depending on the relative weight ratio between acetoxy-PDMS and starch, a certain amount of starch granules was initially dispersed in heptane (~20 mL) and sonic processed for a few minutes using a 500 W probe sonicator (VC 505, Sonics & Materials Inc.) at 40% amplitude. The resulting slurry was then mixed vigorously into the viscous acetoxy-PDMS, Elastosil E43 resin. The use of heptane was necessary to reduce the resultant starch–resin mixture viscosity. The original viscosity of acetoxy-PDMS is 3×10^5 cP, which is close to the thixotropic level and is difficult to mold without liquid injection molding at high pressures. Once the concentration of starch granules in acetoxy-PDMS exceeds 15%, free flow of the resulting paste is no longer possible. Heptane can be added during the mixing of starch granules into acetoxy-PDMS through mechanical stirring or a priori as a vehicle carrying dispersed starch granules as described above. The resultant pastes were degassed in a low vacuum desiccator for 5 min, carefully stirred again to avoid potential sedimentation, and poured into 120 mm side square polystyrene molds where they were left to cure overnight under ambient conditions. The viscosity of the slurries was adjusted to a honeylike consistency (~2500 cP) just before molding to make the pouring/molding easy with little shrinkage. For this reason, the starch concentration in heptane dispersions was generally varied from 0.4 to 0.8 mg/mL, which corresponds to the lowest and highest starch content in the final elastomer, respectively. This approach enables the production of bioelastomers containing up to 80% unmodified starch granules by weight. We should note that because of differences between the density of starch (0.7 g cm^{-3}) and acetoxy-PDMS (1.03–1.1 g cm^{-3}), the corresponding volume fraction of starch is higher in the final bioelastomer. For instance, 30, 50, 70, and 80% starch measured by weight have corresponding volume percent values of 46, 66, 82, and 89%, respectively.

To test the compatibility of starch granules with addition-cured polysiloxane chemistry, we used a standard two-part PDMS (Sylgard 184, Dow Corning) that contains vinyl-terminated polysiloxanes and methylhydrosiloxanes as parts one and two that are catalyzed by an organometallic Pt complex catalyst.[24] An identical mixing procedure as described above was followed for the bioelastomers obtained from addition-cured PDMS (siloxy-PDMS). To distinguish the bioelastomers from one another, the acetoxy-PDMS bioelastomers will be referred to as E-type and the siloxy-PDMS bioelastomers as S-type.

The morphology of the E-type elastomers was investigated with a JEOL JSM-6490LA scanning electron microscope equipped with a tungsten thermionic electron source operated in high vacuum mode with an acceleration voltage of 30 kV. To image the morphology of the cross sections, ruptured samples obtained from mechanical stress–strain tests were used (see below for details). The surfaces were sputter coated with a thin carbon layer (~5 nm) to increase conductivity and enhance imaging contrast. Infrared spectra of the samples were obtained with an attenuated total reflection (ATR) accessory (MIRacle ATR, PIKE Technologies) coupled to a Fourier transform infrared (FTIR) spectrometer (Equinox 70 FT-IR, Bruker). All spectra were recorded in the range from 3800 to 600 cm^{-1} with 4 cm^{-1} resolution, accumulating 128 scans. In a typical measurement, the sample was gently placed on the spot of the ATR accessory and slowly pressed. To ensure the reproducibility of the obtained spectra, three samples from each type were measured.

Bulk mechanical properties of the E-type elastomers were evaluated by uniaxial tensile tests on dog bone-shaped samples (4 mm width, 1 mm thickness, 25 mm length) with an Instron 3365 dual column testing machine. The sample stretching rate was adjusted according to the type of sample on the basis of preliminary tests with 10 mm min^{-1} for rigid specimens (high starch content) and 100 mm min^{-1} for specimens exhibiting large elongation. The elastic modulus, ultimate tensile strength, and elongation at break were extracted from the stress–strain curves. Additionally, energy dissipation and stress relaxation properties were recorded from cyclic tensile tests on samples (5 mm width, 1 mm thickness, 10 mm starting length) with a custom designed Deben miniaturized dual-screw uniaxial tensile stage with a strain cycling rate of 5 mm min^{-1} and a strain value from ~0.1 to 0.4–0.8 (depending on the elongation at fracture of each specimen). Energy dissipation was evaluated from the area beneath the stress–strain curve of a complete load–unload cycle. A normalized dissipation energy factor (η) was defined as the area of each hysteresis loop over the elastic energy at the corresponding maximum strain (eq 1).[26]

$$\eta = \frac{\oint \sigma \, d\varepsilon}{\int_{\varepsilon_{min}}^{\varepsilon_{max}} \sigma \, d\varepsilon} \tag{1}$$

where η denotes the dissipation factor, σ is the stress, and ε is the strain. Additionally, stress relaxation values were extracted from the normalized variation of peak stress values at each cycle as a function of the number of cycles.

Surface characterization was performed in detail on the S-type elastomers, as the type of polysiloxane chemistry (Slygard PDMS) used is highly relevant for applications in microfabrication and microfluidics. However, both E- and S-type bioelastomers had identical wetting properties. Specifically, wetting properties of the bioelastomers were measured using a contact angle goniometer. Three microliters of water droplets were placed at random locations on the bottom surface of each sample. The bottom surface, which was in contact with the mold, was chosen for the wetting measurements because it was free from solvent evaporation-related surface imperfections that might be present on the elastomer–air interface. The reported contact angle values were obtained from an average of 20 measurements. Water uptake properties of the bioelastomers were measured by immersing the samples in deionized water and monitoring the weight change of each sample at different immersion time intervals. Prior to the immersion tests, the samples were kept in a controlled humidity environment (40 ± 5% relative humidity) for at least 2 weeks and then carefully weighed prior to immersion. Weight changes were initially recorded every 30 min, and then every day, so that both short and long term water uptake dynamics could be monitored.

The surface tribological properties of the bioelastomers were evaluated through friction coefficient measurements, which were performed on a CSM Instruments micro combi scratch tester by applying a constant normal load of 200 mN on a Rockwell 0.1 mm diameter sphero-conical diamond tip moving laterally at a rate of 1 mm min^{-1} on the specimen surface. The friction coefficient was calculated as the ratio between the recorded lateral force and the applied normal load. Three repetitions were conducted for each sample and averaged.

Biodegradability was evaluated on selected samples through a standard biochemical oxygen demand (BOD) test that is an indirect and nonspecific test that evaluates mineralization by measuring the amount of oxygen consumed during a degradation reaction.[27] The tests were performed on E-type elastomers containing 30 and 70% starch by weight. For each sample, three measurements were collected. Carefully weighed samples (200 mg) were finely minced and immersed in 432 mL bottles containing seawater collected from the Genoa area shoreline. The solutions in the bottles were stirred with magnetic anchors for 60 days in the dark, mimicking the pelagic marine environment.[27] Oxygen consumed through biodegradation reactions was recorded at different time intervals by the sealed OxiTop caps on each bottle that can monitor changes in oxygen levels. BOD from blank bottles filled with only seawater was also measured for reference. The decrease in the oxygen levels was related to starch consumption through stoichiometry of the general aerobic degradation reaction (eq 2).[27]

$$C_nH_aO_bN_c + \left(n + \frac{a}{4} - \frac{b}{2} - \frac{3c}{4}\right)O_2 \rightarrow nCO_2 + \left(\frac{a}{2} - \frac{3c}{2}\right)H_2O + cNH_3 \tag{2}$$

where $C_nH_aO_bN_c$ represents the organic compound that would biodegrade, consuming $n + a/4 - b/2 - 3c/4$ moles of oxygen. The moles of consumed oxygen divided by the molecular weight of the

DOI: 10.1021/am508515z
ACS Appl. Mater. Interfaces 2015, 7, 3742–3753

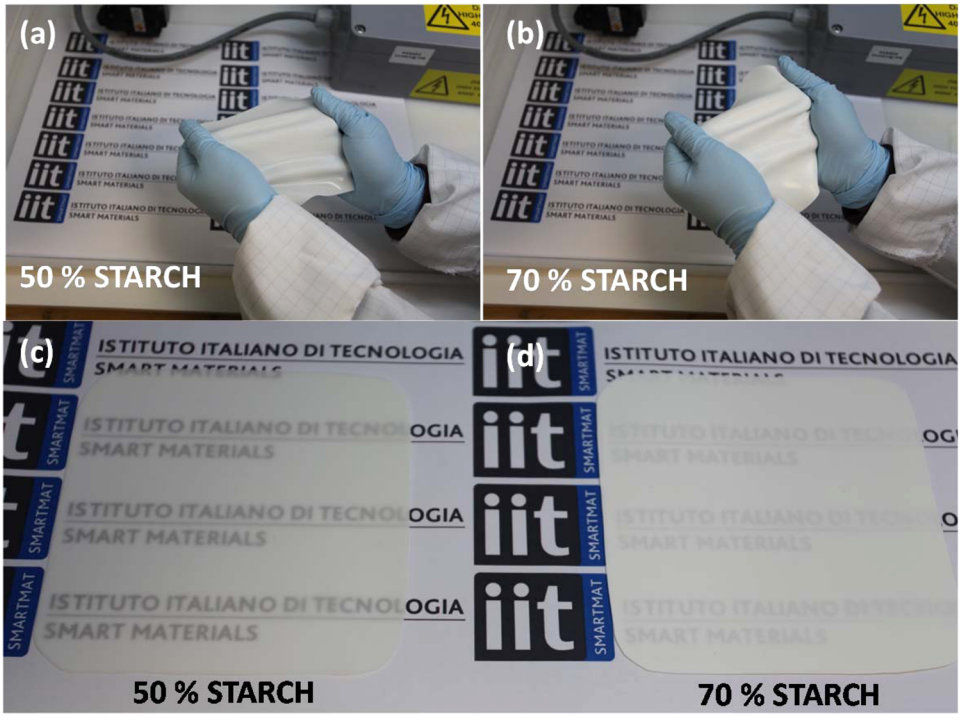

Figure 1. Photographs of bioelastomers containing (a) 50 and (b) 70% unmodified corn starch granules. Photographs indicate that the bioelastomers with (c) 50 and (d) 70% starch are somewhat transparent when placed on a flat surface, which macroscopically indicates a good degree of starch particle dispersion.

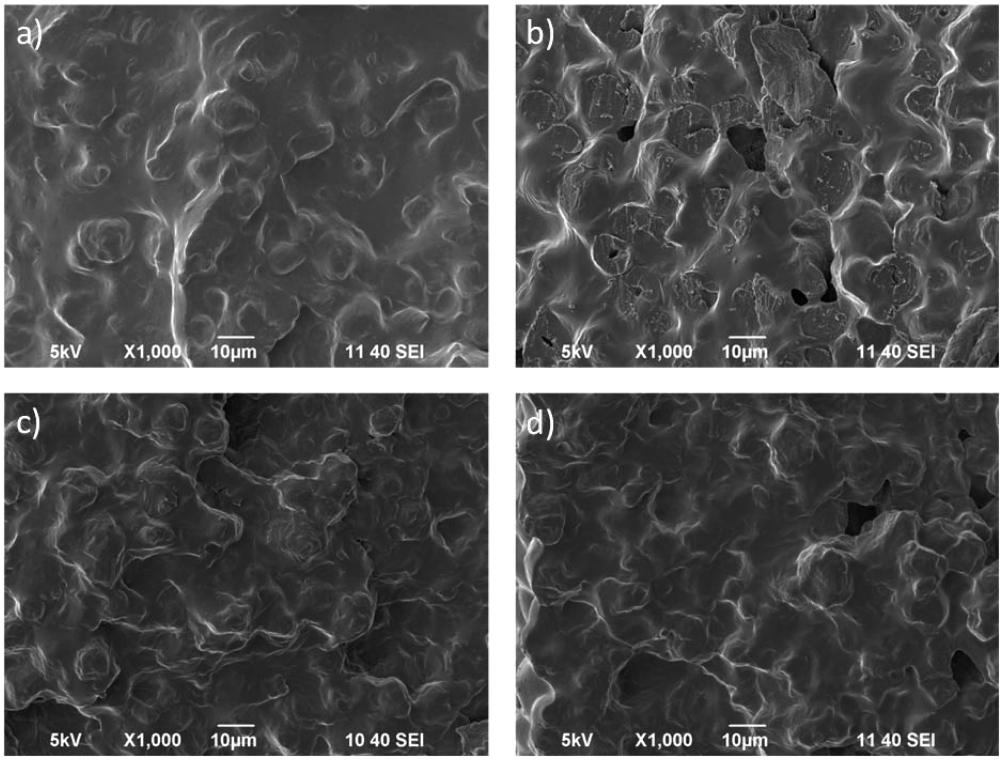

Figure 2. Scanning electron microscope images of cross sections of the E-type bioelastomers containing (a) 30, (b) 50, (c) 70, and (d) 80% starch granules by weight.

organic compound and multiplied by the molecular weight of oxygen represents the oxygen consumption in mg of O_2 per mg of compound. According to Krupp and Jewel,[26] the theoretical BOD value for starch (the oxygen needed for complete degradation) is 1.07 mg of O_2 per mg of starch. They also indicated that a nondegrading matrix containing 40% starch (for instance) would have a BOD value of 0.4 × 1.07 = 0.43. In calculations pertaining to our bioelastomers, we have treated the cross-linked PDMS network as a nondegrading matrix considering the time frame of the experiments (60 days). Moreover, measurements from control bottles containing starch-free E- and S-

DOI: 10.1021/am508515z
ACS Appl. Mater. Interfaces 2015, 7, 3742−3753

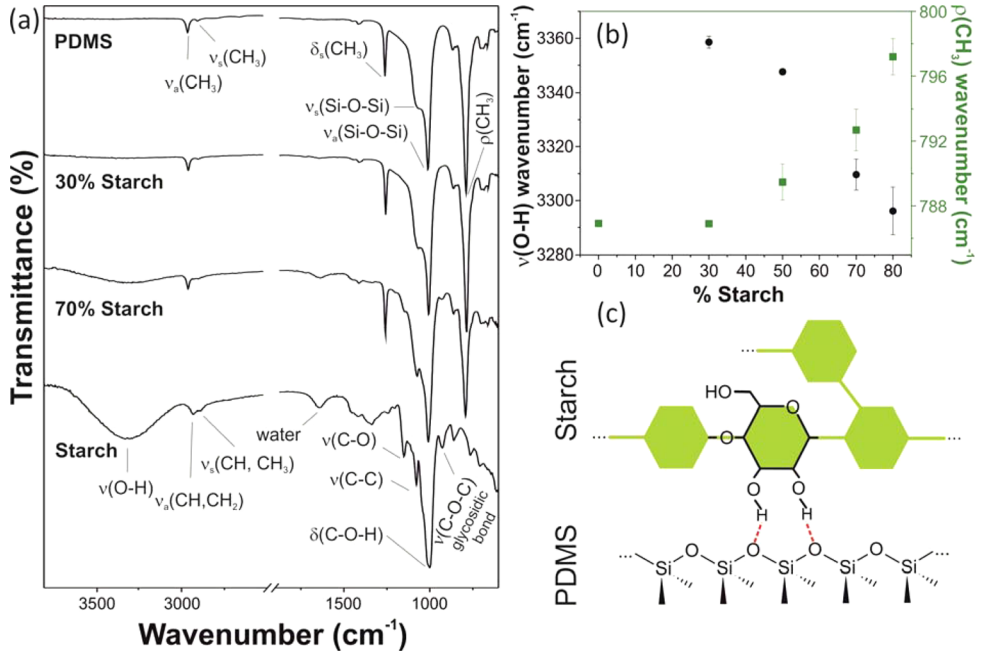

Figure 3. (a) ATR-FTIR (3750−600 cm^{-1}) spectra of acetoxy-PDMS and bioelastomers with 30 and 70% starch contents. (b) Variation of the position of O−H stretching (black circles) and CH_3 rocking vibrations (green squares) at various starch concentrations. (c) Schematic representation of proposed hydrogen bond interactions (red dashed lines) between the starch granules and PDMS polymeric chains.

type PDMS networks indicated insignificant changes in the oxygen levels, confirming that they can be considered nondegrading matrices. However, note that PDMS networks, including uncross-linked PDMS oligomers and silicone oils, are considered nontoxic and are known to be biodegraded by various bacteria and enzymes available in sweet and salty waters.[28−30]

Given the widespread use of PDMS as a support for cell culture,[31−33] biocompatibility of the bioelastomers was also evaluated. Cell adhesion and proliferation tests were conducted on S-type bioelastomers with 30, 50, and 70% unmodified starch content for 7 days, using human osteosarcoma cells (HOS, Cell Bank ICLC) cultured in Dulbecco's Modified Eagle's medium. This medium contains a high concentration of amino acids and vitamins as well as additional supplements including 10% fetal bovine serum and 2 mM L-glutamine. Cells were fixed and stained with diamidino-2-phenylindole (DAPI), which is a blue fluorescent probe that upon selectively binding to the minor groove of double stranded DNA fluoresces ∼20-fold greater than in the unbound state. Its selectivity for DNA and high cell permeability allows for efficient staining of cell nuclei with little background from the cytoplasm. The cytoskeleton of the cells was stained with fluorescein phalloidin, which is a high affinity F-actin probe conjugated to the green fluorescent dye fluorescein (FITC−phalloidin). Cell viability was qualitatively evaluated via conventional fluorescence microscopy (Nikon Eclipse 80i).

RESULTS AND DISCUSSION

Figure 1 shows photographs of E-type bioelastomers (∼350 μm thick) containing 50% (Figure 1a) and 70% (Figure 1b) unmodified corn starch. The photographs in Figure 1c and d indicate that the starch granules maintain a very good degree of dispersion within the cross-linked polysiloxane network as evidenced by the slightly transparent nature of the elastomers once they are laid flat on a surface. The excellent compatibility between starch granules and the acetoxy-PDMS network can be attributed to the interaction of the starch surface with siloxanes and silanes.[34] Starch surfaces in contact with silanes are sometimes referred to as silylated starches. This surface interaction or coupling renders starch hydrophobic and enables its reactive blending with other thermoplastics polymers.[35,36] Moreover, in the case of E-type bioelastomers, the acetic acid byproduct can functionalize starch granule surfaces.[36] Acetic acid-treated starches are generally converted to acetylated starches and are known to have better compatibility with hydrophobic matrices and silicone moieties as well as better dispersion and thermal stability when incorporated into hydrophobic thermoplastics.[37,38]

The microscale cross section morphology of the E-type bioelastomers is shown in Figure 2 as a function of increasing starch concentration from 30 to 80% by weight. As seen, there appears to be no significant differences in the morphologies of the bioelastomers at different starch concentrations. This suggests that starch granules disperse very well within the polysiloxane network prior to cross-linking regardless of their initial concentration. The texture of the features in the cross sectional images in the form of micrometer scale bumps (∼10 μm) is attributed to dispersed starch granules that are well embedded within the PDMS network even at the highest starch concentration (Figure 2d). Very similar morphologies were found for the S-type bioelastomers as well. The absence of large starch agglomerates within the bioelastomers under such a wide range of concentrations indicates that during mixing a strong interfacial interaction in the form of coupling between the unmodified corn scratch granules and the polysiloxanes and acetoxysilanes is established with subsequent cross-linking. In fact, starch particle surface functionalization with various silanes to improve interfacial strength and subsequent dispersion has been shown to successfully reinforce various rubber matrices.[38] However, in the present case, such interactions occur naturally because both the rubbery matrix and the coupling agents consist of polysiloxanes and acetoxysilanes (E-type) or siloxysilanes (S-type).

E-type bioelastomers were characterized by ATR-FTIR measurements as shown in Figure 3a. Acetoxy cross-linked PDMS network films not containing any starch granules

DOI: 10.1021/am508515z
ACS Appl. Mater. Interfaces 2015, 7, 3742−3753

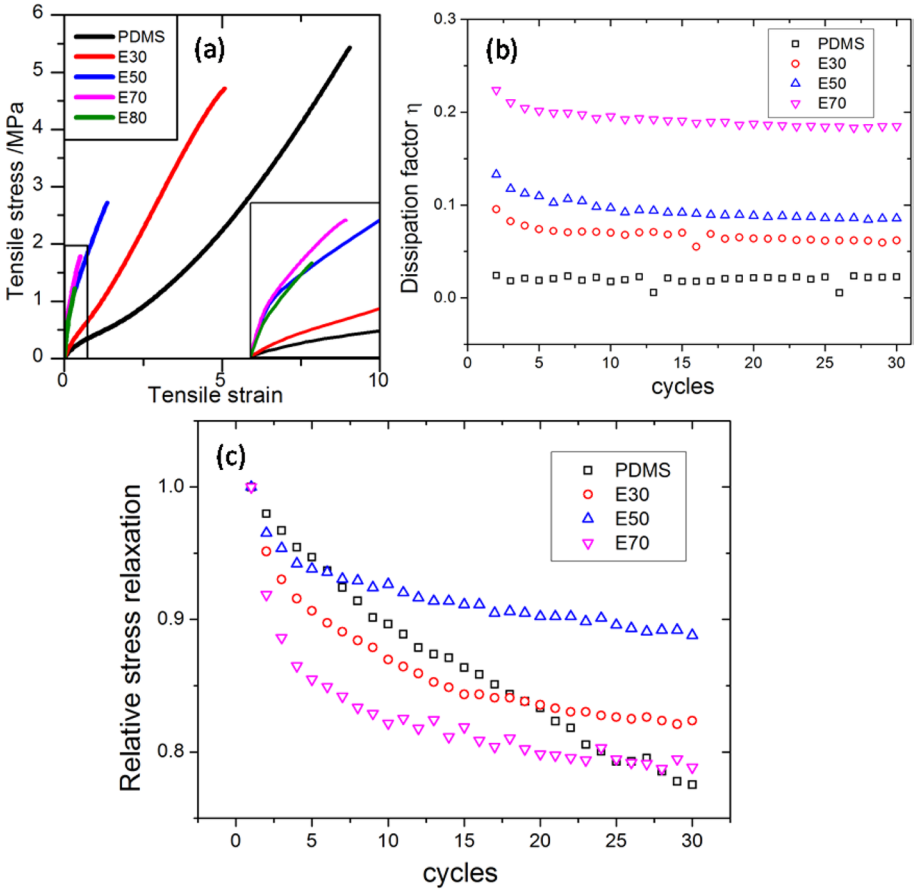

Figure 4. (a) Stress–strain measurement results for acetoxy-PDMS and E-type bioelastomers. The notations E30, E50, E70 and E80 stand for bioelastomers containing 30, 50, 70, and 80% unmodified starch granules, respectively. (b) Calculated mechanical energy dissipation factors obtained from 30 cyclic stress–strain experiments. (c) Stress relaxation results obtained from the same cyclic stress–strain tests for bioelastomers containing 30, 50, and 70 unmodified starch.

displayed characteristic peaks at 2963 and 2905 cm^{-1}, which can be assigned to CH_3 asymmetric and symmetric stretching, respectively. The peak appearing at 1260 cm^{-1} is assigned to CH_3 symmetric bond bending, and the peaks at 1063 and 1009 cm^{-1} are assigned to Si–O–Si symmetric and asymmetric band stretching, respectively. Finally, the peak at 796 cm^{-1} is assigned to CH_3 band rocking.[39] Conversely, the main bands due to the corn starch spectrum are O–H stretching at 3313 cm^{-1} and asymmetric and symmetric stretching of C–H and CH_2 bands at 2932 and 2889 cm^{-1}, respectively. The adsorbed water band appears at 1645 cm^{-1}. C–O and C–C stretching modes with different degrees of interaction with water appear at 1150 and 1001 cm^{-1}. A C–O–H bending signal is found at 1078 cm^{-1}, and the C–O–C glycosidic bond appears at 928 cm^{-1}.[40−42]

FTIR spectra of the E-type bioelastomers did not exhibit the formation or disappearance of new or existing chemical bands relative to those of the pure components (Figure 3a). However, two significant shifts related to the positioning of the O–H stretching of starch and the CH_3 rocking of PDMS were observed as shown in Figure 3b. The position of the O–H stretching band of starch within the elastomers was shifted to a lower wavenumber, from 3359 cm^{-1} at a starch concentration of 30% (E30) to 3296 cm^{-1} for 80% starch (E80), indicating a shift of 63 cm^{-1}. Usually, this size of effect is related to bonding interactions via hydrogen bond bridges.[43] Moreover, the CH_3 rocking vibration of PDMS is shifted to a somewhat higher wavenumber as the starch concentration was increased from 787 cm^{-1} for 0% starch to 797 cm^{-1} for 80% starch. Such a shift in this band pertaining to methyl groups has been related to changes in the electronegativity and modification of atomic distances along the bond.[44] These changes are known to originate from the formation of new hydrogen bonds in interacting systems. In this case, for instance, new hydrogen bonds are formed between the hydroxyl groups of starch and the oxygen of the siloxane groups of the cross-linked PDMS network, as schematically shown in Figure 3c. This inductive interaction is expected to get more intense with increasing concentrations of starch that modify not only the Si–O–Si bond via hydrogen bonding but also the apparent electronegativity of the Si atoms and the distance between the silicon and methyl groups ($Si–CH_3$) along the PDMS chains. All of these modifications can in turn significantly alter the ordering of the PDMS segments within the bioelastomers. Molecular dynamics simulations showed that such alterations significantly affect the transport (heat, mechanical energy, and electrical) and interfacial properties of PDMS networks.[45] Similar interactions have been measured between starch and the siloxy-PDMS network.

Mechanical Characterization. The stress–strain characteristics of the E-type bioelastomers are shown in Figure 4a. Because of the different modes of cross-linking possibilities, the mechanical properties of PDMS elastomers can span from soft gels to stiff elastomers.[46] The nonlinear stress–strain behavior

DOI: 10.1021/am508515z
ACS Appl. Mater. Interfaces 2015, 7, 3742−3753

Table 1. Summary of Mechanical, Surface Wetting, and Friction Properties of the Bioelastomers

		bulk mechanical properties (E materials)				surface (S) properties	
sample	starch (wt %−vol %)	E (MPa)	elongation at break (%)	UTS (MPa)	dissipation factor η	contact angle (deg)	friction coefficient μ
PDMS	0−0	0.87 ± 0.06	885 ± 91	4.68 ± 0.57	0.020 ± 0.05	120	0.72 ± 0.01
E30/S30	30−46	1.08 ± 0.04	500 ± 19	4.69 ± 0.11	0.062 ± 0.001	122	0.35 ± 0.01
E50/S50	50−66	7.54 ± 3.33	132 ± 69	2.54 ± 0.38	0.086 ± 0.001	124	0.39 ± 0.01
E70/S70	70−82	8.62 ± 0.38	53 ± 2	1.80 ± 0.15	0.185 ± 0.001	141	0.45 ± 0.01
E80	80−89	6.25 ± 0.14	90 ± 77	1.20 ± 0.10			

of the acetoxy-PDMS cross-linked network (0% starch concentration) shows a brief linear elastic region up to a strain level of 0.5 (50% elongation). This region is marked by a rectangle in Figure 4a, which is expanded in the inset. A recent study by Palchesko et al.[46] showed that the Young's modulus of various types of PDMS elastomers can be extracted from this initial strain region on the basis of the strong nonlinear elongation properties of silicone rubbers. Beyond this region, nonlinear elastic stretching occurs with increasing elastic constant. This stress−strain region up a strain level of 5 (500%) has the highest nonlinearity, which can be attributed to the stretching-induced alignment of entangled, cross-linked siloxane units along the direction of stretching, and is followed by more linear behavior that can possibly be attributed to collectively aligned chain extension until the rubber finally ruptures at a strain level of ∼8.85 (885%). Note that deformation of the acetoxy-PDMS cross-linked network resembles biological soft tissues such as skin,[46−49] which have J-shaped stress−strain curves. Although the unfilled acetoxy-PDMS elastomer has a stress-stain curve that appears to be somewhat J-shaped, elastomers that have been developed to simulate soft tissues produce an almost constant (slightly increasing) tensile stress response until a certain stress level is reached, which is known as the typical J-shape.[50] It is not possible to describe such soft elastic materials with a single Young's modulus. Attempts to model J-shaped elastic stretching of soft materials using Neo-Hooke models have been reported, but they are beyond the scope of this work. However, the Young's modulus can generally be used as an indicator when it corresponds to the low strain region .[48] For the bioelastomers containing 30% unmodified starch granules, stretching characteristics that are due to the acetoxy-PDMS network no longer prevail, and the final rupture strain value declines to 5 (500%). The material displays an almost Hookean stress−strain behavior with slight nonlinearity, which is possibly due to limited alignment of free entangled units along the direction of stretching.

Increasing the starch granule concentrations further results in strain rupture values at and below 1.25 (125%) that closely resemble rigid (Hookean) solids. In other words, as shown in Figure 4a, increasing starch content results in decreased elongation at break because the rigidity of starch becomes much higher than that of the PDMS chains, leading to disappearance of the J-shape. In fact, when the starch content is higher than 50%, it does not look like an elastomer but rather looks more like a linear elastic. This observation should be clarified. The Young's modulus of the elastomers increases as a function of increased starch granule concentration from 0.87 MPa (corresponding to the low strain zone for acetoxy-PDMS) to 8.6 MPa, which is increased almost ten times for the bioelastomers containing 70% starch granules as shown in Table 1. At the same time, the ultimate tensile strength (UTS) of the bioelastomers decreases as a function of increasing starch concentration from nearly 9 to 0.5, corresponding to unfilled acetoxy-PDMS and 70% starch concentration (see Table 1). Above 70% starch concentration, a slight decrease in the Young's modulus was measured, which can be attributed to onset of the loss of binding and encapsulating ability of the cross-linked PDMS polymer network over each and every corresponding starch granule because of the high volume of the granules with respect to siloxanes. Electron microscopy images of the newly exposed surfaces from the ruptured samples (see Figure 2) showed that failure, especially at starch concentrations ≤30%, involves rupture of the PDMS matrix with negligible fracture points on the starch particles or delamination or separation of the starch/PDMS interface. This confirms the existence of a good degree of physicochemical compatibility and miscibility between the cross-linked matrix and the starch granules.

Despite differences in the stress−strain behavior and the elastic response as a function of starch concentration, E-type bioelastomers were found to have high elastic recovery rates and low loss of mechanical properties (i.e., low degree of irreversible viscous deformations as evidenced by the cyclic stress relaxation measurements shown in Figure 4c). Compared to pure acetoxy-PDMS elastomers, starch-containing elastomers displayed higher initial relaxation rates based on the slopes fitted to early cycle relaxation data, which was followed by stabilization after ∼20 cycles in constrast to the acetoxy-PDMS elastomers, which did not reach a stable value by the end of the test (30 cycles). This suggests a potential reduction in the mobility of the PDMS segments in the interfacial regions of starch granules and the PDMS network, which consecutively reduces the overall agility of the cross-linked network to effectively cause "stiffening" of the polymer matrix. This phenomenon is quite common for nanosilica-filled PDMS composites.[48,49] In such a dynamic system under cyclic stress conditions, dispersed starch granules can act as anchor points for the recovery of polymer chain deformations because the PDMS chains are not completely free due to hydrogen bonding interactions with the starch granules (see Figure 3c). Energy dissipation in the bioelastomers (expressed as a dissipation factor) obtained from the same cyclic tests was higher than for the unfilled acetoxy-PDMS network under the strain rates studied (0.1 to 0.4−0.8). Hence, the measured dissipation factors, as shown in Figure 4c, increased as a function of starch granule concentration to a level of 0.2 for the bioelastomers containing 70% starch. This is quite noteworthy as green materials with relatively high modulus and high strain energy dissipation properties are continuously being sought for many industrial applications, including use as shock absorbers in machinery, protection of electronic equipment, and general purpose packaging. To date, only aligned-carbon nanotubes and orderly packed small metal balls embedded in PDMS networks have been shown to be efficient strain energy dissipation materials.[49,50] In summary, the semi-rigid starch particles

DOI: 10.1021/am508515z
ACS Appl. Mater. Interfaces 2015, 7, 3742−3753

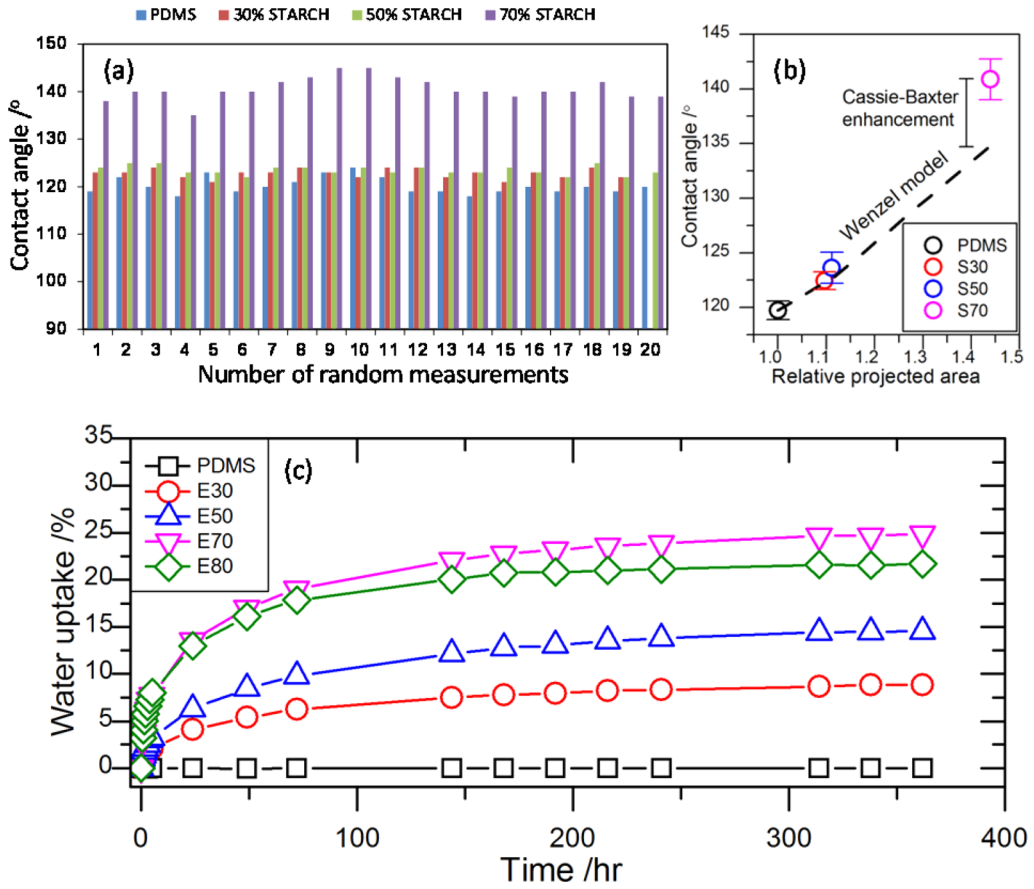

Figure 5. (a) Static water contact angle measurements obtained from 20 different random surface locations on the S-type bioelastomers as a function of starch content. (b) Representation of the wetting measurements as a function of surface roughness plotted using eq 3. Deviation from the Wenzel wetting mode is observed when the starch concentration is 70% by weight. (c) Water uptake measurements for the S-type elastomers immersed in water for two weeks.

dispersed in such polysiloxanes can serve as physical cross-linking points to provide certain observed properties, such as tunable elasticity and lowered friction coefficients.

Water Interaction and Low Friction. As mentioned earlier, unmodified starch particles also display excellent compatibility with vinyl-terminated polysiloxanes and siloxysilanes that form PDMS networks via addition cross-linking reactions. Siloxy-PDMS networks are not as elastic as acetoxy-PDMS networks, but they are used extensively in microfabrication and microfluidics due to their acetic acid-free cross-linking. Therefore, wetting studies and surface tribology measurements are presented for S-type bioelastomers. Note that identical wetting characteristics were measured for the E-type bioelastomers but are not shown here for brevity. Static water contact angle measurements are shown in Figure 5a. Twenty random measurements were made on each sample surface to gauge the uniformity of the wetting properties. The calculated standard deviations for siloxy-PDMS and 30, 50, and 70% starch-containing surfaces were 1.69, 0.94, 0.92, and 2.23°, respectively, indicating coherent surface chemistry and wetting properties. The average static contact angles for each surface are reported in Table 1. Even though starch is hydrophilic and highly prone to surface water adsorption, the bioelastomers became more hydrophobic as the unmodified starch concentration was increased. This intrinsically suggests that regardless of the starch granule concentration the granule surfaces are effectively coupled and encapsulated by the cross-linked PDMS network, leaving no exposed starch at the elastomer surface, which would be reflected by much larger standard deviations in the contact angle measurements. Moreover, the surface roughness measurements indicated that starch granules increased the surface roughness of the PDMS network considerably. The surface RMS (root-mean-square) roughness of the unfilled PDMS network was measured to be 30 nm, whereas the surface roughnesses of the 30, 50, and 70% bioelastomers were measured to be much larger, namely, 1.58, 1.65, and 1.75 μm, respectively. The relationship between the measured contact angle on a rough surface (θ^*) compared to its smooth counterpart (θ) is given by the classical Cassie–Baxter equation[51]

$$\cos \theta^* = r_f f \cos \theta + f - 1 \quad (3)$$

where f represents the fraction of the area that is wetted by the liquid and r_f (roughness ratio) is the ratio between the true area of the solid surface to the apparent wetted area. When $f = 1$, the drop wets all of the surface asperities, and the dashed line in Figure 5b shows the wetting trend following eq 3 when $f = 1$, which represents the Wenzel model.[52] The contact angle data clusters very close to this dashed line following the Wenzel mode of wetting. Note that bioelastomers with starch content less than 70% follow the Wenzel wetting mode as shown in Figure 5b, whereas the average static contact angle measured for the 70% starch bioelastomer does not fall on the Wenzel line but rather can be approximated by the Cassie–Baxter

DOI: 10.1021/am508515z
ACS Appl. Mater. Interfaces 2015, 7, 3742–3753

wetting mode with $f \approx 0.77$ and is close to 150°, which is regarded as the onset of superhydrophobicity. Starch-based biopolymers are prone to high levels of water uptake. Therefore, it is of interest to evaluate the water uptake characteristics of the bioelastomers developed in this study. Figure 5c shows the water uptake measurements of E-type bioelastomers that were observed continuously under water for up to 2 weeks. The unfilled acetoxy-PDMS network shows negligible water uptake, whereas 30 and 50% starch-containing elastomers saturate at approximately 8 and 12% water uptake levels, respectively. These levels are considered quite satisfactory because they are less than half the water uptake levels of TPS[53,54] over a similar time period. Water uptake values for bioelastomers with 70 and 80% unmodified starch concentrations saturate at approximately 22 and 24%, respectively, which are levels that are still less than TPS. It is worth mentioning that the time needed to reach steady state water uptake levels, ~2 weeks, is also longer than the values reported in most studies concerning TPS,[53−55] which range from 3 to 8 days.

Surprisingly, starch granules were found to lower the friction coefficient of the siloxy-PDMS network considerably as shown in Figure 6. Lowering of the PDMS surface friction coefficient

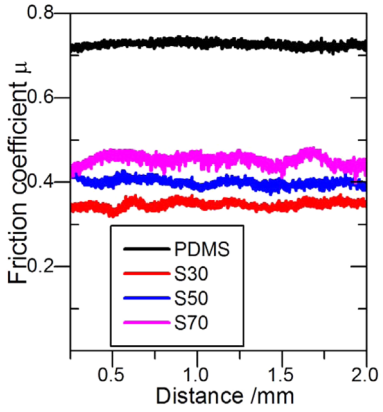

Figure 6. Comparison of friction coefficient values as a function of horizontal displacement obtained under a 200 mN load for bioelastomers containing 0% (PDMS), 30% (S30), 50% (S50), and 70% (S70) unmodified starch granules embedded in the siloxy-PDMS network.

is extremely important, particularly for biomedical applications.[56] Until recently, friction was considered to be controlled by only surface chemistry and structure. However, this was shown not to be true for soft materials, such as rubbers and gels, where the friction of the soft matter involves the bulk effects.[57,58] Viscoelastic deformation of soft materials can be the major result of energy dissipation associated with friction. It naturally follows that enhanced surface hydrophobicity and roughness should reduce the friction coefficient because of fewer chemical interactions as well as reduced solid−solid contact frequency. However, friction between solid surfaces is a direct result of how contact-generated shear stresses are distributed and dissipated along the surface. As shown in Figure 4b, the bioelastomers have good bulk stress relaxation behavior. This inherent property can also take place as surface stress relaxations generated due to friction and enhanced surface hydrophobicity can collectively reduce the friction coefficient when starch granules are introduced into the siloxy-PDMS network. As such, the bioelastomers display friction coefficient values (see Figure 6) that are much lower than those of commercial rubbery materials such as acrylonitrile−butadiene rubbers[57,59] and are comparable to those of lubricated, microtextured PDMS surfaces[58−60] without requiring a lubricant.

Biodegradation and Biocompatibility. Figure 7 shows biochemical oxygen demand (BOD_{60}) measurements for E-type bioelastomers containing 30% (Figure 7a) and 70% starch (Figure 7b) immersed in bottles containing seawater for 60 days. In the first 10 days, the oxygen gas consumption for both samples was negligible compared to that of the control bottles containing only seawater. After this period, however, the amount of oxygen consumed (in mg) for both samples started and continued to increase until the end of the two month trial. The bioelastomer with the 30% starch concentration had an increase in oxygen consumption that resembled an exponential rise (a red line is included as a guide), whereas the oxygen consumption of the bioelastomer with 70% starch concentration increased in a linear fashion. At the end of the 60 days, the bioelastomer with 70% starch concentration consumed approximately three times more oxygen, indicating faster biodegradation kinetics. The insets in Figure 7 show the fluctuating oxygen consumption data for unfilled acetoxy-PDMS matrices that averaged around 0.5 mg between 30 and 60 days and can be considered as negligible compared to the bioelastomers. At the end of the test, the BOD_{60}'s of the bioelastomers with 30 and 70% starch concentrations were 0.027 and 0.051 mg oxygen per mg of starch, respectively. Note that both values are calculated by subtracting the baseline measurements of oxygen consumption in the seawater-alone control experiment. Once the concentration of oxygen consumed is determined experimentally, it can be converted to moles of oxygen consumed. Then, using the model oxidation reaction given by eq 2, the corresponding number of moles of degraded starch can be estimated. For the specific test conditions studied herein, only 2.5 and 5% of the initial volume of bioelastomers was degraded in the seawater for the samples containing 30 and 70% starch, respectively, after 60 days. Although degradation kinetics are strongly affected by the bacterial and enzymatic conditions of the degradation medium, based on the present measurements made on pulverized samples in the dark, we project that it would take approximately 3−6 years for the bioelastomers to completely degrade in Mediterranean seawater without accounting for acetoxy-PDMS degradation dynamics.

The bioelastomers were also found to be thoroughly biocompatible, rendering them suitable for various biomedical applications. Figure 8 shows the interaction of human osteosarcoma cells with the S-type bioelastomer surfaces, including the unfilled control PDMS sample after 7 days in culture. Cell nuclei are stained blue with DAPI, whereas the cell cytoskeletons are stained green with FITC−Phalloidin. The cells were observed to be proliferating, have a healthy appearance, and have a good degree of cytoplasmic extension in all of the samples studies. Future work will include more detailed and statistical analyses of different cell cultures. Note that starch autofluorescence is increasingly noticeable in the microscopy images as the starch concentration increases (Figure 8).

CONCLUSIONS

We present a facile method to fabricate mechanically robust bioelastomers from unmodified corn starch granules by

DOI: 10.1021/am508515z
ACS Appl. Mater. Interfaces 2015, 7, 3742−3753

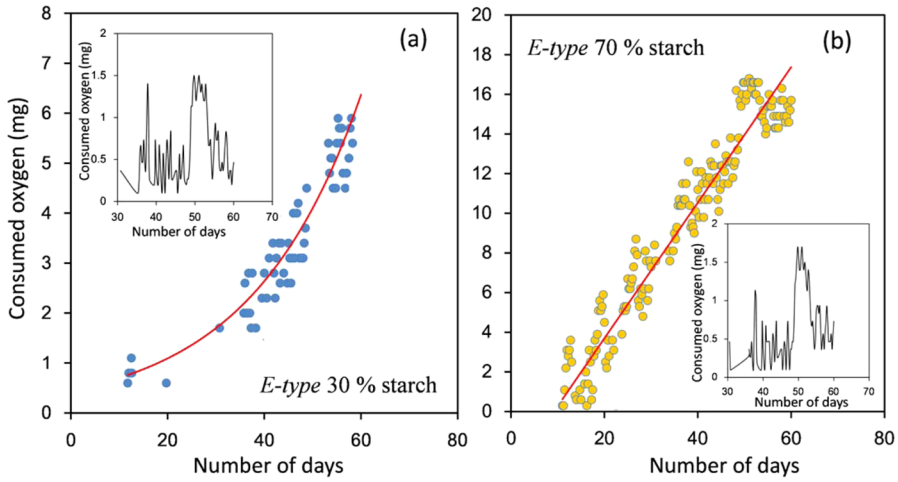

Figure 7. (a) Oxygen consumption data for E-type bioelastomers with 30% starch content immersed in Mediterranean seawater maintained in the dark for 60 days. (b) Oxygen consumption data for E-type bioelastomers with 70% starch content immersed in Mediterranean seawater maintained in the dark for 60 days. (insets) Oxygen consumption of acetoxy-PDMS with no starch as control. Within the first 10−12 day period, no measurable consumption of oxygen gas was detected.

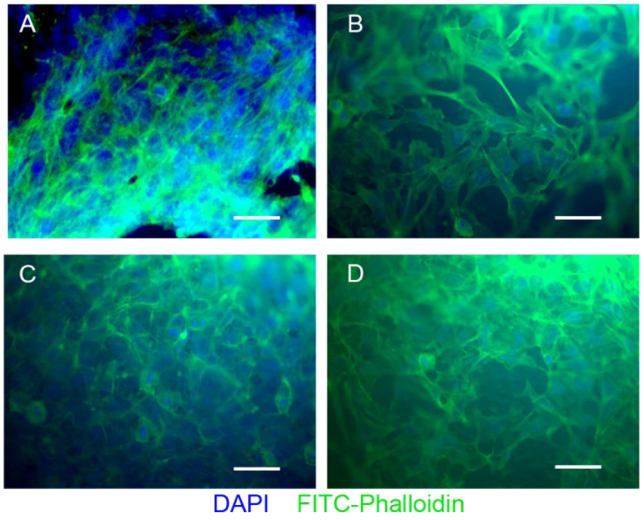

Figure 8. Human osteosarcoma (HOS) cells on (A) PDMS, (B) S30, (C) S50, and (D) S70 after 7 days in culture. Cell nuclei (blue) are marked with DAPI, and the cell cytoskeleton (green) with FITC−Phalloidin. Scale bars represent 50 μm. Cell proliferation was observed in all samples. The increasingly saturated background is attributed to starch autofluorescence.

dispersing them in common acetoxy- and siloxy-cured polysiloxane resins under ambient conditions. The mechanical properties of the bioelastomers can be tuned from rigid to soft and stretchable by carefully adjusting the concentration of the starch granules. The degree of dispersion of starch granules within the polysiloxane networks was excellent and was maintained by simple mixing even with starch loading exceeding 70% by weight. This is attributed to starch particle surface functionalization by polysiloxanes and silanes before and during the cross-linking reactions. Bioelastomers displayed excellent mechanical stress relaxation and energy dissipation properties compared to unfilled PDMS networks, suggesting that they are sustainable substitutes for mechanical energy dampeners. Their surfaces were found to be hydrophobic, and the hydrophobicity was enhanced by increasing the starch granule concentrations. Starch also decreased surface friction coefficients that were correlated to the collective effects of good bulk stress damping properties, enhanced surface hydrophobicity, and roughness. Compared to thermoplastic starch, the bioelastomers displayed water uptake values that were much lower with longer immersion times under water. Experiments conducted in Mediterranean seawater enabled estimation of biodegradation times ranging from 3 to 6 years depending on the percentage of starch content. The use of nanosized starch particles will be considered in future studies.

AUTHOR INFORMATION

Corresponding Author

*E-mail: ilker.bayer@iit.it.

Notes

The authors declare no competing financial interest.

ACKNOWLEDGMENTS

We thank Mrs. Nga Tran, Smart Materials, Istituto Italiano di Technologia for assistance with some of the experiments. Mrs. Alice Scarpellini is also acknowledged for assistance with electron microscopy

REFERENCES

(1) Lörcks, J. Properties and Applications of Compostable Starch-Based Plastic Material. *Polym. Degrad. Stab.* **1998**, *59*, 245−249.
(2) Liu, H.; Xie, F.; Yu, L.; Chen, L.; Li, L. Thermal Processing of Starch-Based Polymers. *Prog. Polym. Sci.* **2009**, *34*, 1348−1368.
(3) Jane, J.-L. Current Understanding on Starch Granule Structures. *J. Appl. Glycosci.* **2006**, *53*, 205−213.
(4) Lu, D. R. Starch-Based Completely Biodegradable Polymer Materials. *eXPRESS Polym. Lett.* **2009**, *3*, 366−375.
(5) van Soest, J. J. G.; Benes, K.; de Wit, D.; Vliegenthart, J. F. G. The Influence of Starch Molecular Mass on the Properties of Extruded Thermoplastic Starch. *Polymer* **1996**, *37*, 3543−3552.
(6) Thunwall, M.; Boldizar, A.; Rigdahl, M. Compression Molding and Tensile Properties of Thermoplastic Potato Starch Materials. *Biomacromolecules* **2006**, *7*, 981−986.
(7) Müller, C. M. O.; Yamashita, F.; Laurindo, J. B. Evaluation of the Effects of Glycerol and Sorbitol Concentration and Water Activity on the Water Barrier Properties of Cassava Starch Films through a Solubility Approach. *Carbohydr. Polym.* **2008**, *72*, 82−87.

DOI: 10.1021/am508515z
ACS Appl. Mater. Interfaces 2015, 7, 3742−3753

(8) Halley, P.; Rutgers, R.; Coombs, S.; Kettels, J.; Gralton, J.; Christie, G.; Jenkins, M.; Beh, H.; Griffin, K.; Jayasekara, R.; Lonergan, G. Developing Biodegradable Mulch Films from Starch-Based Polymers. *Starch - Stärke* **2001**, *53*, 362−367.
(9) Yu, L.; Dean, K.; Li, L. Polymer Blends and Composites from Renewable Resources. *Prog. Polym. Sci.* **2006**, *31*, 576−602.
(10) Sarazin, P.; Li, G.; Orts, W. J.; Favis, B. D. Binary and Ternary Blends of Polylactide, Polycaprolactone and Thermoplastic Starch. *Polymer* **2008**, *49*, 599−609.
(11) Wang, L.; Shogren, R. L.; Carriere, C. Preparation and Properties of Thermoplastic Starch−Polyester Laminate Sheets by Coextrusion. *Polym. Eng. Sci.* **2000**, *40*, 499−506.
(12) Huneault, M. A.; Li, H. Morphology and Properties of Compatibilized Polylactide/Thermoplastic Starch Blends. *Polymer* **2007**, *48*, 270−280.
(13) Willett, J. L. Mechanical Properties of Ldpe/Granular Starch Composites. *J. Appl. Polym. Sci.* **1994**, *54*, 1685−1695.
(14) Griffin, G. J. L. Biodegradable Synthetic Resin Sheet Material Containing Starch and a Fatty Material. U.S. Patent 4,016,117, 1977.
(15) Chandra, R.; Rustgi, R. Biodegradation of Maleated Linear Low-Density Polyethylene and Starch Blends. *Polym. Degrad. Stab.* **1997**, *56*, 185−202.
(16) Kim, S.; Peterson, S. C. Development of Degradable Polymer Composites from Starch and Poly(ethyl cyanoacrylate). *Polym. Compos.* **2012**, *33*, 904−911.
(17) de Buyl, F. Silicone Sealants and Structural Adhesives. *Int. J. Adhes. Adhes.* **2001**, *21*, 411−422.
(18) Lehmann, R. G.; Varaprath, S.; Frye, C. L. Degradation of Silicone Polymers in Soil. *Environ. Toxicol. Chem.* **1994**, *13*, 1061−1064.
(19) Lehmann, R. G.; Miller, J. R.; Kozerski, G. E. Degradation of Silicone Polymer in a Field Soil under Natural Conditions. *Chemosphere* **2000**, *41*, 743−749.
(20) Sabourin, C. L.; Carpenter, J. C.; Leib, T. K.; Spivack, J. L. Biodegradation of Dimethylsilanediol in Soils. *Appl. Environ. Microbiol.* **1996**, *62*, 4352−4360.
(21) Lehmann, R. G.; Miller, J. R. Volatilization and Sorption of Dimethylsilanediol in Soil. *Environ. Toxicol. Chem.* **1996**, *15*, 1455−1460.
(22) Daniels, A. Silicone Breast Implant Materials. *Swiss Med. Wkly.* **2012**, *142*, 13614−13626.
(23) Curtis Jim, C. A., Medical Applications of Silicones. In *Biomaterials Science: An Introduction to Materials in Medicine*, 2nd ed.; Elsevier: Burlington, MA, 2004.
(24) Gelest. http://www.gelest.com/Goods/Pdf/Reactivesilicones.pdf.
(25) Koratkar, N. A.; Suhr, J.; Joshi, A.; Kane, R. S.; Schadler, L. S.; Ajayan, P. M.; Bartolucci, S. Characterizing Energy Dissipation in Single-Walled Carbon Nanotube Polycarbonate Composites. *Appl. Phys. Lett.* **2005**, *87*, 063102−063105.
(26) Krupp, L. R.; Jewell, W. J. Biodegradability of Modified Plastic Films in Controlled Biological Environments. *Environ. Sci. Technol.* **1992**, *26*, 193−198.
(27) Tosin, M.; Weber, M.; Siotto, M.; Lott, C.; Degli Innocenti, F. Laboratory Test Methods to Determine the Degradation of Plastics in Marine Environmental Conditions. *Front. Microbiol.* **2012**, *3*, 225−231.
(28) Anderson, C.; Hochgeschwender, K.; Weidemann, H.; Wilmes, R. Studies of the Oxidative Photoinduced Degradation of Silicones in the Aquatic Environment. *Chemosphere* **1987**, *16*, 2567−2577.
(29) Neu, T. R.; Van der Mei, H. C.; Busscher, H. J.; Dijk, F.; Verkerke, G. J. Biodeterioration of Medical-Grade Silicone Rubber Used for Voice Prostheses: A Sem Study. *Biomaterials* **1993**, *14*, 459−464.
(30) Genchi, G. G.; Ciofani, G.; Liakos, I.; Ricotti, L.; Ceseracciu, L.; Athanassiou, A.; Mazzolai, B.; Menciassi, A.; Mattoli, V. Bio/Non-Bio Interfaces: A Straightforward Method for Obtaining Long Term PDMS/Muscle Cell Biohybrid Constructs. *Colloids Surf., B* **2013**, *105*, 144−151.
(31) Leclerc, E.; Sakai, Y.; Fujii, T. Cell Culture in 3-Dimensional Microfluidic Structure of Pdms (Polydimethylsiloxane). *Biomed. Microdevices* **2003**, *5*, 109−114.
(32) Di Carlo, D.; Wu, L. Y.; Lee, L. P. Dynamic Single Cell Culture Array. *Lab Chip* **2006**, *6*, 1445−1449.
(33) Kaur, B.; Ariffin, F.; Bhat, R.; Karim, A. A. Progress in Starch Modification in the Last Decade. *Food Hydrocolloids* **2012**, *26*, 398−404.
(34) Kim, E. G.; Kim, B. S.; Kim, D. S. Physical Properties and Morphology of Polycaprolactone/Starch/Pine-Leaf Composites. *J. Appl. Polym. Sci.* **2007**, *103*, 928−934.
(35) Jariyasakoolroj, P.; Chirachanchai, S. Silane Modified Starch for Compatible Reactive Blend with Poly(lactic acid). *Carbohydr. Polym.* **2014**, *106*, 255−263.
(36) Tarvainen, M.; Sutinen, R.; Peltonen, S.; Tiihonen, P.; Paronen, P. Starch Acetate—a Novel Film-Forming Polymer for Pharmaceutical Coatings. *J. Pharm. Sci.* **2002**, *91*, 282−289.
(37) Roopa, S.; Premavalli, K. S. Effect of Processing on Starch Fractions in Different Varieties of Finger Millet. *Food Chem.* **2008**, *106*, 875−882.
(38) Elzein, T.; Galliano, A.; Bistac, S. Chains Anisotropy in PDMS Networks Due to Friction on Gold Surfaces. *J. Polym. Sci., Part B: Polym. Phys.* **2004**, *42*, 2348−2353.
(39) Tang, H.; Qi, Q.; Wu, Y.; Liang, G.; Zhang, L.; Ma, J. Reinforcement of Elastomer by Starch. *Macromol. Mater. Eng.* **2006**, *291*, 629−637.
(40) Kizil, R.; Irudayaraj, J.; Seetharaman, K. Characterization of Irradiated Starches by Using Ft-Raman and FTIR Spectroscopy. *J. Agric. Food Chem.* **2002**, *50*, 3912−3918.
(41) Wilson, R. H.; Belton, P. S. A Fourier-Transform Infrared Study of Wheat Starch Gels. *Carbohydr. Res.* **1988**, *180*, 339−344.
(42) Bellamy, L. J. *The Infrared Spectra of Complex Molecules*; Springer: Netherlands, 1980.
(43) Takenaka, T. Effect of Adjacent Groups on the Symmetrical Cd_3 Deformation Frequencies. *Bull. Inst. Chem. Res. Kyoto Univ.* **1962**, *40*, 191−191.
(44) Tsige, M.; Soddemann, T.; Rempe, S. B.; Grest, G. S.; Kress, J. D.; Robbins, M. O.; Sides, S. W.; Stevens, M. J.; Webb, E. Interactions and Structure of Poly(dimethylsiloxane) at Silicon Dioxide Surfaces: Electronic Structure and Molecular Dynamics Studies. *J. Chem. Phys.* **2003**, *118*, 5132−5142.
(45) Khanafer, K.; Duprey, A.; Schlicht, M.; Berguer, R. Effects of Strain Rate, Mixing Ratio, and Stress-Strain Definition on the Mechanical Behavior of the Polydimethylsiloxane (PDMS) Material as Related to Its Biological Applications. *Biomed. Microdevices* **2009**, *11*, 503−508.
(46) Palchesko, R. N.; Zhang, L.; Sun, Y.; Feinberg, A. W. Development of Polydimethylsiloxane Substrates with Tunable Elastic Modulus to Study Cell Mechanobiology in Muscle and Nerve. *PLoS One* **2012**, *7*, e51499.
(47) Schneider, F.; Draheim, J.; Kamberger, R.; Wallrabe, U. Process and Material Properties of Polydimethylsiloxane (PDMS) for Optical Mems. *Sens. Actuators, A* **2009**, *151*, 95−99.
(48) Wagner, S.; Lacour, S. P.; Jones, J.; Hsu, P.-h. I.; Sturm, J. C.; Li, T.; Suo, Z. Electronic Skin: Architecture and Components. *Physica E* **2004**, *25*, 326−334.
(49) Misra, A.; Kumar, P. Periodic Architecture for High Performance Shock Absorbing Composites. *Sci. Rep.* **2013**, *3*, 2056−2065.
(50) Misra, A.; Raney, J. R.; De Nardo, L.; Craig, A. E.; Daraio, C. Synthesis and Characterization of Carbon Nanotube−Polymer Multilayer Structures. *ACS Nano* **2011**, *5*, 7713−7721.
(51) Cassie, A. B. D.; Baxter, S. Wettability of Porous Surfaces. *Trans. Faraday Soc.* **1944**, *40*, 546−551.
(52) Wenzel, R. N. Surface Roughness and Contact Angle. *J. Phys. Colloid Chem.* **1949**, *53*, 1466−1467.
(53) Gáspár, M.; Benkő, Z.; Dogossy, G.; Réczey, K.; Czigány, T. Reducing Water Absorption in Compostable Starch-Based Plastics. *Polym. Degrad. Stab.* **2005**, *90*, 563−569.

DOI: 10.1021/am508515z
ACS Appl. Mater. Interfaces 2015, 7, 3742−3753

(54) Mathew, A. P.; Dufresne, A. Plasticized Waxy Maize Starch: Effect of Polyols and Relative Humidity on Material Properties. *Biomacromolecules* **2002**, *3*, 1101−1108.
(55) Corradini, E.; Carvalho, A. J. F. d.; Curvelo, A. A. d. S.; Agnelli, J. A. M.; Mattoso, L. H. C. Preparation and Characterization of Thermoplastic Starch/Zein Blends. *Materials Research* **2007**, *10*, 227−231.
(56) Abbasi, F.; Mirzadeh, H.; Katbab, A.-A. Modification of Polysiloxane Polymers for Biomedical Applications: A Review. *Polym. Int.* **2001**, *50*, 1279−1287.
(57) Persson, B. N. J. On the Theory of Rubber Friction. *Surf. Sci.* **1998**, *401*, 445−454.
(58) He, B.; Chen, W.; Jane Wang, Q. Surface Texture Effect on Friction of a Microtextured Poly(dimethylsiloxane) (PDMS). *Tribol. Lett.* **2008**, *31*, 187−197.
(59) Huang, W.; Jiang, L.; Zhou, C.; Wang, X. The Lubricant Retaining Effect of Micro-Dimples on the Sliding Surface of PDMS. *Tribol. Int.* **2012**, *52*, 87−93.
(60) Chawla, K.; Lee, S.; Lee, B. P.; Dalsin, J. L.; Messersmith, P. B.; Spencer, N. D. A Novel Low-Friction Surface for Biomedical Applications: Modification of Poly(dimethylsiloxane) (PDMS) with Polyethylene Glycol(Peg)-Dopa-Lysine. *J. Biomed. Mater. Res., Part A* **2009**, *90*, 742−749.

DOI: 10.1021/am508515z
ACS Appl. Mater. Interfaces 2015, 7, 3742−3753